Pulse Width Modulation for Simulating Time-Dependent Quantum Systems

Qi-Ming Chen[1,2] and Re-Bing Wu[†1,2]
[1)] *Department of Automation, Tsinghua University, Beijing, 100084, China*
[2)] *Center for Quantum Information Science and Technology, TNList, Beijing, 100084, China*[a)]

This paper proposes a numerical method for solving time-dependent Schrödinger equations with finite spectral bandwidth, which applies to both periodic and non-periodic cases. We introduce the concept of Pulse Width Modulation (PWM), which is broadly used in classical control engineering, to simulate time-dependent quantum dynamics by switching between a finite number of constant Hamiltonians. The switching timings can be programmed to improve the precision and save computational resources. The effectiveness of the PWM method is demonstrated by numerical simulations, which shows that it is faster and more robust than the standard piecewise constant control systems. Moreover, we also propose the realization of PWM method for potential implementation in experimental systems.

I. INTRODUCTION

Precise and efficient simulation of quantum dynamics is expected to lead to profound insights in physics as well as to novel applications[1]. For a quantum system governed by the time-dependent Hamiltonian $\hat{H}(t)$, its state evolution obeys the Schrödinger equation (SE) and has the formal solution

$$|\psi(t)\rangle = \hat{U}(t,0)|\psi_0\rangle = \hat{T}\exp\Big(-i\int_0^t \hat{H}(t')dt'\Big)|\psi(0)\rangle,$$

where $|\psi(t)\rangle$ is the system state at time t, $\hat{T}$ is Dyson time-ordering operator (or Magnus time-ordering operator when $\int_0^t \hat{H}(t')dt' < \pi$). However, seeking an exact solution of a given SE is usually not available[2], and even approximately solving this problem for a wide parameter range has been proved to be extremely hard and complex[3]. How to accurately and effectively simulating a quantum system is thus crucial for understanding the properties of the system and exploring its further applications.

Quantum Simulation (QS) emerges for experimentally simulating a quantum system by quantum mechanics means, including Digital Quantum Simulation (DQS), Analogue Quantum Simulation (AQS), and Quantum-Information-Inspired Algorithms (QIIA)[4]. DQS usually relays on Trotter formula[5], and aims to simulating universal time-independent systems through a sequence of single and two-qubit gates[6–8]; time-dependent systems have only been investigated recently[9,10]. AQS relays on seeking mappings from a simulated system to a controllable one[11], which is however looked simple to do difficult; nevertheless, due to the advantage in relatively easy measurement, it continues to attract more and more interests though the past 10 years[12,13]. QIIA is developed recently for simulating many-body quantum systems, which usually combines with Monte Carlo techniques to efficiently calculate physical quantizes[14,15].

Though QS merits an absolute advantage in solving SE in high-dimensional cases, a simple mathematical algorithm nevertheless is much more feasible than that for the many cases we usually encountered. For weak-coupling systems, the Time-Dependent Perturbation Theory (TDPT) is regarded as a standard technique, and the Rotating Wave Approximation (RWA) is widely accepted when the system is also in or near resonance[16,17]. The case of strong-coupling systems is much more complex. For "two-level atom with periodically driven fields", Barata *et al.* proposed a strong-coupling expansion when external fields are free of secular terms[18]; Irish *et al.* proposed a matrix diagonalization method to find the eigenvalues and eigenfunctions when the frequency detuning is extremely large[19]; Wu *et al.* proposed an iterative method that can convert the problem into an iteration of weak-coupling problems[3]. When the Hamiltonian contains only linear potential, accurate solutions are available by using the Lewis and Riesenfeld Invariant Method (LR)[20], which can be further modified that leads to a more general solution[21,22];in addition, there are also other methods which contain Airy Function[23] or Wei-Norman Theorem[24]. When the Hamiltonian contains nonlinear potentials, the methods usually depend highly on suitable configurations[25], which may not be easily reviewed in this paper.

In practice, many time-dependent Hamiltonians display periodic patterns, e.g. systems driven by continuous waves or electromagnetic fields, so that approaches focusing on periodic systems play the most important role in solving SE. Shirley introduced the Floquet Theory (FT) that transfers the SE with a periodic Hamiltonian into an equivalent one with infinite dimensional time-independent Hamiltonian[26], which can be improved by perturbation approach to avoid the "infinite" problem[27]; Haeberlen *et al.* based on Magnus Expansion and proposed the Average Hamiltonian Theory (AHT) for seeking unitary propagator[28]; Mananga *et al.* fused the two methods and proposed the Floquet-Magnus Expansion (FME) that simplifies the calculation and shows advantages in various circumstances[29].

[a)] Electronic mail: rbwu@tsinghua.edu.cn

Under most circumstances, one has to design computational algorithms to construct a numerical solution[30]. Piecewise Constant Scheme (PWC) is to break up the total evolution operator into small increments of time duration τ in which the variation of the Hamiltonian operator is negligible, so that the propagator from t to $t+\tau$ can be approximated by

$$\hat{U}(t+\tau,t) = \exp\Big[-i\tau\hat{H}(t+\frac{\tau}{2})\Big], \qquad (1)$$

where the sampling point $t+\frac{\tau}{2}$ is decided by the Exponential Midpoint Rule that usually guarantees a result with the highest precision among PWC schemes[31]. Though it requires very small steps τ to be stable in numerical scheme[30], this approach is broadly used in quantum control studies for its obvious simplicity; moreover, the piecewise constant controls can be directly implemented in many practical cases. Besides, there are also other strategies to calculate the propagator. One approach is based on various polynomial expansion of the propagator: the Second Order Differencing (SOD) focus on accurately calculating time derivatives with Taylor expansion[32,33]; the Chebyshev Method (CH) seeks the optimal polynomial expansion to the propagator (in CH the τ can be very large)[34,35]; the Short Iterative Lanczos Propagation (SIL) projects the propagator onto the so called Krylov subspace and generates a finite polynomial expansion[36]. Another approach is based on the Trotter formula for factorizing the exponential form of the propagator[5]: Feit and Fleck first introduced the Split Operator Method (SPO) and developed a high accuracy spectral method[37], then they provided a useful method for determining the eigenvalues and eigenfunctions[38]; Suzuki and Bandrauk *et al.* further developed SPO and pushed it to a higher precision, which shows a distinct advantage in quantum simulation[39,40].

Different from all the schemes mentioned above where error is analysed in high-order polynomial terms of τ, we proposed a rather convenient method where the error lies in high-frequency terms outside a chosen scope, saying Pulse Width Modulation (PWM). The idea of transferring the approximation error into frequency domain can be traced to very early works, where Fast Fourier Transformation (FFT) has been introduced to calculate derivatives to improve the calculation accuracy[33,37]. If approximation is unavoidable in the simulation of quantum dynamics, neglecting high-order terms in frequency domain may be always much more economic than neglecting those in time domain. This is also what behind RWA where it keeps only the slowest terms in weak-coupling and near-resonance situation; the PWM method we presented in this paper is much more general as higher-order terms can be kept for much wider applicabilities, including weak and strong coupling, periodic and non-periodic, low and high dimensional cases.

The rest of this paper is organised as follows. In Sec. II, we introduce the Pulse Width Modulation (PWM) and show how a time-dependent Hamiltonian can be transformed into the PWM form; in Sec. III, we provide a priori error formula to estimate the possible error induced by PWM transformation, and discussed what factors that influence the accuracy; in Sec. IV, we compare the computational complexity between PWM and PWC, and analyses how PWM accelerates simulating quantum dynamics. To combine PWM with experimental quantum simulation, we discuss in Sec. V the robustness of PWM pulses with noise on the pulse width to mimic the possible laboratorial condition; we illustrate in Sec. VI other possible realizations of PWM transformation, e.g. Gaussian pulse train, to explore its applicability in quantum control experiments. Finally, we summarise all the results and draw the conclusions in Sec. VII.

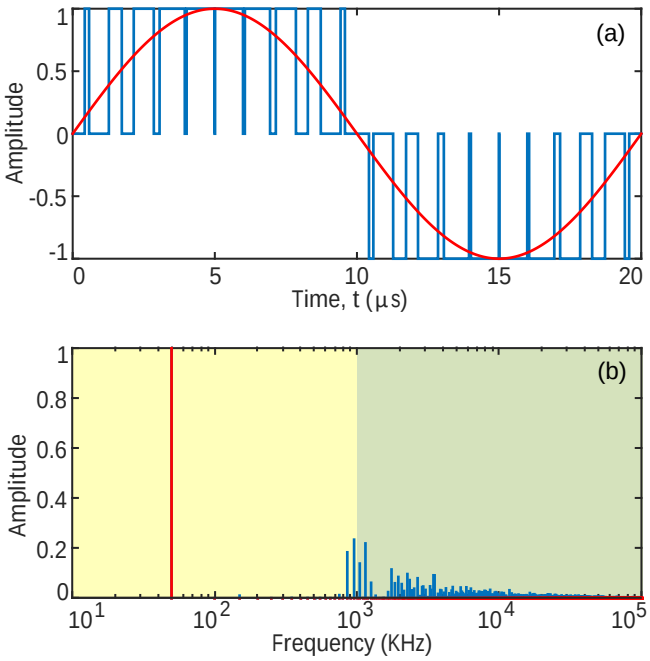

FIG. 1. (Color online) Schematics for PWM transformation. (a), (b) Time-dependent function $\sin\omega t$ of frequency $\omega = 50$KHz (red) and the corresponding 20-step PWM form (blue) in time domain and in frequency domain, respectively. The areas within and without the frequency scope $\Omega = 1$MHz are distinguished by yellow and green color, respectively.

II. BASIC CONCEPTS OF PWM

The strategy of PWM is to transform the time-dependent Hamiltonian into a sequence of time-independent ones, called the PWM form, which can be diagonalized before and repeatedly used throughout the calculation. For example

$$\{\hat{H}_0 + u(t)\hat{H}_1\} \leftrightarrow \{\hat{H}_0,\ \hat{H}_0 \pm \xi\hat{H}_1\}$$

where ξ is a constant called pulse amplitude. The name PWM is a well accepted concept in control technology in power electronics[41,42], which is based on the fact that any function $u(t)$ with finite frequency bandwidth can be well approximated at any precision by a sequence of rectangular pulses with unanimous amplitude $\xi = \max_t |u(t)|$ but different pulse width t_p. To apply PWM to a quantum system, we define the Frequency Band $\Delta = [\omega_{min}, \omega_{max}]$ as the interval from the minimum to the maximum frequency of all the time-dependent variables in the Hamiltonian, and the Frequency Scope $\Omega = M\omega_{min}$ as the frequency limit one should care about, where M is called the Pulse Number within every time interval $2\pi/\omega_{min}$. Consider an arbitrary time-dependent Hamiltonian in the semiclassical form

$$\hat{H}(t) = \hat{H}_0 + \sum_{k=1}^{K} u_k(t)\hat{H}_k, \tag{2}$$

where H_0 and H_k's are time-independent Hamiltonians, $u_k(t)$'s are time-dependent real functions with finite bandwidth, i.e.

$$u_k(t) = \frac{1}{\pi}\int_{\omega_{min}}^{\omega_{max}} d\omega A_k(\omega)\sin\Big(\omega t + \phi_k(\omega)\Big). \tag{3}$$

The transformation of Eq. (2) into its PWM form is operated by transforming the real functions $u_k(t)$'s into a sequence of rectangular pulses. For a superposition of M rectangular functions which are centered at $(m-1/2)\tau$ for $m = 1, \cdots M$ and $\tau = T/M$, with identical period $T = 2\pi/\omega_{min}$ and amplitude ξ but different pulse width $t_{p,k}^{(m)}$, it can be Fourier expanded as

$$\tilde{u}_k(t) = \frac{\xi}{T}\sum_{m=1}^{M} t_{p,k}^{(m)} + \sum_{n=-\infty, n\neq 0}^{+\infty}\Big[\sum_{m=1}^{M}\frac{\xi}{n\pi} \times \sin\Big(\frac{t_{p,k}^{(m)}}{\tau}\frac{n\pi}{M}\Big)e^{-in\omega_{min}(m-\frac{1}{2})\tau}\Big]e^{in\omega_{min}t}. \tag{4}$$

Exactly equating Eq. (3) and (4) is usually impossible; to equate these two terms within frequency scope $\Omega = M\omega_{min}$, one should properly choosing the every pulse width by (see App. A for derivation)

$$t_{p,k}^{(m)} = \xi^{-1}\int_{m\tau}^{(m+1)\tau} dt' u_k(t').$$

Since the formula implies that the pulse areas in each time interval τ should be equal to those of $u_k(t)$, we name it Equal Integral Area Principle (EAP) for further discussion.

In this way, we transform the time-dependent Hamiltonian into the PWM form

$$\hat{H}(t) = \hat{H}_0 + \sum_{k=1}^{K} s_k(t)\xi_k\hat{H}_k, \tag{5}$$

where $s_k(t) \equiv 0, \pm 1$ is a sign function which can be regarded as a sequence of unitary pulses, the default pulse amplitude is set to $\xi_k = \max_t |u_k(t)|$ if without further declaration. Then, one can construct a corresponding time-independent SE in each interval and finally combine the results to construct the solution of the time-dependent SE, for example

$$\hat{U}(t+\tau, t) = \exp\Big[-i\tau(H_0 + u(t+\frac{\tau}{2})\hat{H}_1)\Big] \leftrightarrow$$
$$\hat{U}_M(t+\tau, t) = \exp\Big[-it_f\hat{H}_0\Big]\exp\Big[-it_p(H_0 \pm \xi\hat{H}_1)\Big] \times \exp\Big[-it_f\hat{H}_0\Big],$$

where $t_p = \xi^{-1}\int_t^{t+\tau} dt' u(t')$, $t_f = (\tau - t_p)/2$, subscript M means it is calculated by PWM transformation.

Actually, the concept of EAP lies in nearly all the methods for calculating $\hat{U}(t+\tau, t)$, and can be derived in various ways. For example, when we keep the only 1st-order terms in Magnus expansion, the approximated propagator can be present as

$$\hat{U}(t+\tau, t) \approx \exp\Big[-i\Big(\tau\hat{H}_0 + \Big(\int_t^{t+\tau} dt' u(t')\Big)\hat{H}_1\Big)\Big],$$

which exactly meets EAP. Equivalently, PWC approximates the integral by using the midpoint rule, while PWM by using rectangular pulses. However, in order to emphasis on the frequency properties of PWM, especially to introduce the important concept of frequency scope Ω, we achieved the EAP through Fourier and anti-Fourier transformation.

According to EAP, the frequency properties of PWM transformation remain (nearly) unchanged if one simultaneously raise the pulse amplitude ξ and shrink the pulse duration t_p by the same factor. In the extreme case where $\xi \to \infty$, the 2nd-order SPO can be derived as a special case of PWM

$$\hat{U}_S(t+\tau, t) = \exp(-i\frac{\tau}{2}\hat{H}_0)\exp(\pm i\tau\hat{H}_1)\exp(-i\frac{\tau}{2}\hat{H}_0),$$

where the subscript S means it is calculated by SPO. On the other hand, PWC can also be obtained when allowing the pulse amplitudes vary from different interval. As we will see, a well designed PWM simulation is usually more accurate than SPO, and more efficient than PWC.

III. ERROR ANALYSIS

To evaluate the accuracy of PWM approximation, we introduce the error function

$$\varepsilon(t) = \frac{1}{2}\Big|1 - \langle\psi(t)|\hat{U}_M(t,0)|\psi(0)\rangle\Big|,$$

which is usually called the "infidelity" in quantum information[1]. According to the derivation of PWM, it can be approximated by the following formula

$$\varepsilon_p(t) = \frac{\sqrt{2}}{\pi}\Big|\sum_{k=1}^{K}\int_{\omega_{min}}^{\omega_{max}} d\omega \int_0^t dt' \langle\psi(t')|\hat{H}_k|\psi(t')\rangle \cos\Big[\Big(\omega t' + \phi_k(\omega)\Big) + \pi/4\Big] \sum_{l=1}^{\infty}(-1)^l \cos\Big[lM\Big(\omega t' + \phi_k(\omega)\Big)\Big]\Big|; \quad (6)$$

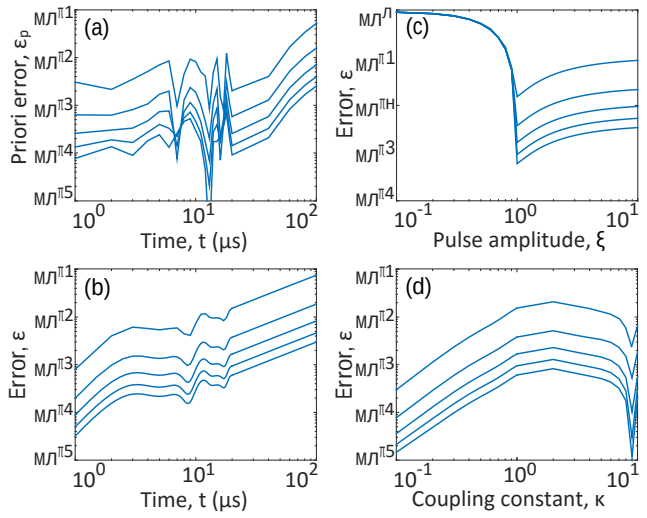

FIG. 2. (Color online) Error Analysis. (a), (b) Estimation error ε_p and actual error ε with evolution time t, respectively (sampled at $2n\mu s$ or $20n\mu s$ for $n = 1, \cdots, 5$). (c), (d) Error ε with pulse amplitude ξ and coupling strength κ_1 at $t = 20\mu s$, respectively (sampled at $0.1n$ or n for $n = 1, \cdots, 10$). From top to the bottom, each line corresponds to a different pulse number $M = 20, \cdots, 100$.

where $\phi_k(\omega) = \pi - \arg\{\int_{-\infty}^{+\infty} dt e^{-i\omega t} u_k(t)\}$ (see App. B for detail). Qualitatively speaking, a small ε_p corresponds to a small coupling constant κ, a small evolution time t, and a large pulse number M, which is consistent with our expectation and will be tested by numerical simulation.

For illustration, we consider the following N-qubit system

$$H = \frac{1}{2^N}\sigma_z^{\otimes N} + \frac{\kappa_1}{2^N}u_1(t)\sigma_x^{\otimes N} + \frac{\kappa_2}{2^N}u_2(t)\sigma_y^{\otimes N}$$

where $\otimes$ is Kronecker product, $\hat{\sigma}_{x,y,z}$ are Pauli operators, $\kappa_{1,2}$ are controllable coupling constants that enable us to switch the system between weak-coupling and strong-coupling regime. For now we set $N = 1$, and consider only one time-dependent variable $u_1(t) = \sin(\omega t)$, which can be described as a spin-$\frac{1}{2}$ particle situated in single external field; we then set $\omega/2\pi = 50$KHz, $\kappa_1 = 1$, $\Omega = 1$MHz, $\xi = 1$, and seek the propagator $\hat{U}(t, 0)$ within one period $t \in [0, 20]\mu s$.

Figure 1(a) shows the relation between $u_1(t)$ and the corresponding PWM pulses. When apply the PWM transformation, we first divide the period into $M = 20$ pieces with $\tau = 1\mu s$; then, we calculated the integral of $u(t)$ in each interval, and obtained the corresponding pulse width t_p by EAP; finally, we calculate the propagator by integrating all the time-independent Hamiltonians explicitly.

Figure 1(b) reveals the properties of the PWM pulses in frequency domain. For the original function $\sin(\omega t)$, the frequency spectrum contains only one peak of unit amplitude at 50KHz; for the PWM pulses, the frequency spectrum contains one peak of unit peak at 50KHz, as well as some small peaks nearly outside scope $\Omega = 1$MHz. This result is highly consistent with our analysis in App. A, which claims a well designed M-step PWM approximation can exactly pick all frequency terms of the original function $u(t)$ within the scope $\Omega = M\omega_{min}$, but leaves small noise outside Ω (see Fig. 7 in supplementary material for more examples).

According to Eq. (6), we derive the estimation error $\varepsilon_p(t)$ for the example

$$\varepsilon_p(t) = \sqrt{2}\Big|\int_0^t dt' \langle\psi(0)|\hat{H}_1(t')|\psi(0)\rangle \times \cos\Big(\omega t' + \frac{\pi}{4}\Big)\sum_{l=1}^{\infty}(-1)^l \cos(M\omega t')\Big|.$$

where

$$\hat{H}_1(t') = \tfrac{1}{2}\hat{U}^\dagger(t', 0)\sigma_x\hat{U}(t', 0), \ |\psi(0)\rangle = [1, 0];$$

Figures 2(a) and (b) respectively show the dependence of estimation error ε_p, as well as actual error ε, on evolution time t. In spite of several singular points caused by the high frequency terms in ε_p, the two errors are always on the same order, saying $\varepsilon_p/\varepsilon \in [0.1, 10]$. For example, at $t = 10\mu s$, $M = 20$, $\varepsilon_p = 7.4 \times 10^{-3}$, $\varepsilon = 8.2 \times 10^{-3}$; at $t = 60\mu s$, $M = 80$, $\varepsilon_p = 4.9 \times 10^{-4}$, $\varepsilon = 2.8 \times 10^{-3}$. This on one hand demonstrates the analysis we made to derive PWM transformation is acceptable; on the other hand, it reveals that the simulation accuracy can be raised by simply increasing the pulse number M, which is also indicated by the estimation error formula. As we will see, a well chosen pulse number M would help speed up computational quantum simulations and make PWM very efficient for calculating propagator in even complex systems.

Figure 2(c) shows the dependence of error ε on pulse amplitude ξ. Despite the area $\xi < \max_t|u(t)|$ (for this example $\max_t|u(t)| = 1$) where EAP cannot always holds, the error ε remains (nearly) unchanged with pulse amplitude $\xi \geq \max_t|u(t)|$. This meets the EAP we derived perviously, saying the result of PWM transformation remains (nearly) unchanged if one simultaneously raise the pulse amplitude and shrink the pulse duration by the same factor. However, due to the approximations we made for deriving EAP, ε in fact increases slightly with ξ, which indicates that $\xi =$

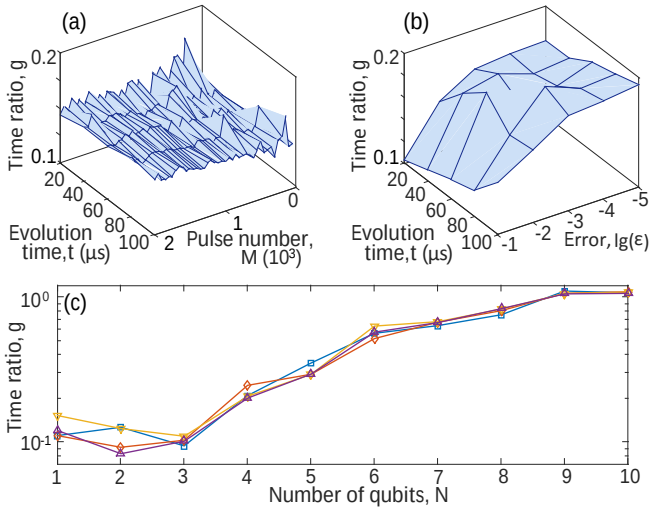

FIG. 3. (Color online) Efficiency analysis. (a), (b) CPU time ratio $g = \frac{t_c|_{PWM}}{t_c|_{PWC}}$ with evolution time t and pulse number M, or with t and accuracy requirement ε, respectively; (c) CPU time ratio g with number of qubits N at evolution time $t = 20\mu s$ with pulse number $M = 50$ (blue), 100 (red), 150 (yellow), and 200 (purple), where nuance of the errors calculated by the two methods are negligible.

$\max_t |u(t)|$ is the optimal choice for simulation. Since the Hamiltonian of the PWM form converges exactly to the 2nd-order SPO form when ξ goes to infinity, we then infer that PWM with any finite pulse amplitude $\xi \geq \max|u(t)|$ is more accurate than 2nd-order SPO under the same number of terms.

Figure 2(d) shows the dependence of error ε on coupling strength κ_1. Different from that in Fig. 2(c) where we simultaneously raise the pulse amplitude and shrink the pulse duration, here we equivalently raise the pulse amplitude by κ_1 but keep the pulse duration unchanged; thus all the frequency components including the undesired noises are equivalently increased by κ_1. In the weak coupling regime $\kappa_1 \leq 1$, ε monotonically increase with coupling constant κ_1; though the error tends to diminish in the strong coupling regime $\kappa_1 \in [1, 10]$, a larger scope of coupling constant κ_1 still shows an increasing tendency. Hence, we conclude that the PWM transformation corresponding to a larger κ_1 will roughly lead to a larger error ε, thus harder to be accurately simulated. To overcome this problem, one has to enlarge the frequency scope Ω (namely increase the pulse number M), and set a smaller interval τ for calculation.

IV. EFFICIENCY ANALYSIS

According to Eq. (5), the propagator of a general system can be present as

$$\hat{U}(t+\tau, t) = \exp\left(-i\tau\left(\hat{H}_0 + \sum_k s_{t,k}\xi_k\hat{H}_k\right)\right),$$

where $\hat{H}_0 + \sum_k s_{t,k}\xi_k\hat{H}_k$ take values only in the following finite set

$$\left\{\hat{H}_0,\ \hat{H}_0 \pm \xi_k\hat{H}_k,\ \hat{H}_0 \pm \xi_{k1}\hat{H}_{k1} \pm \xi_{k2}\hat{H}_{k2},\ \cdots\right\}.$$

For example, one can pre-diagonalize the Hamiltonians $\hat{H}_0 = D_0\Lambda_0 D_0^\dagger$, $\hat{H}_0 \pm \xi H_1 = D_\pm\Lambda_\pm D_\pm^\dagger$, and simplify the propagation by product of constant matrices and exponential of diagonal matrices

$$\begin{aligned}\hat{U}_M(t+\tau, t) = D_0 \exp(-it_f\Lambda_0) D_M \\ \times \exp(-it_p\Lambda_\pm) D_M^\dagger \exp(-it_f\Lambda_0) D_0^\dagger,\end{aligned}$$

where $D_M = D_0 D_\pm$. In other words, PWM transforms the calculation of exponentiations with matrices on the shoulder into exponentiations with only scalars on the shoulder, and thus we expect PWM may simplify the computational complexity and accelerate the simulation of quantum dynamics by a large extent.

Figures 3(a) and (b) show the difference of computational complexity (CPU time t_c) between PWM and PWC for the $N = 1$ example. CPU time t_c represents the minimum computational resource required for simulation[43], which corresponds to the minimum piece number M for both PWM and PWC. Although t_c increases with pulse number M as well as evolution time t for the both methods, PWM always outperforms PWC for saving computational resources. At the same condition pulse number M, PWM shows a $81.6 \sim 89.6\%$ time saving than PWC; at the same condition of error ε, PWM still shows a $78.3 \sim 89.6\%$ time saving. We further increase the dimension of the problem to see the limit of PWM acceleration, Fig. 3(c) shows the dependence of time ratio $g = \frac{t_c|_{PWM}}{t_c|_{PWC}}$ on number of qubits N. On the one hand, the time saving of PWM decreases with qubit number N, e.g. at $N = 2$ (equivalently 4 dimension), PWM roughly saves 99.0% computational time for corresponding evolution; at $N = 8$ (equivalently 256 dimension), PWM saves 16.5% computational time; on the other hand, the small g in higher-dimensional cases in fact saves a larger quantity of computational complexity since calculating time evolution of high-dimensional problems usually requires an extremely long time, e.g. PWM saves $0.01s$ for calculating $\hat{U}(t, 0)$ at $N = 2$, while it saves $0.24s$ at $N = 8$ ($M = 200$). In summary, we claim that PWM is highly efficient for computational quantum simulation, which keeps the approximation error under control throughout a long time interval (see Fig. 8 in supplementary material for more examples).

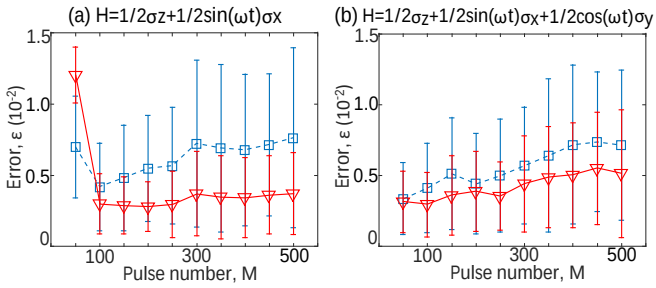

FIG. 4. (Color online) Robustness analysis. (a), (b) Error ε and standard variance under switching noise with pulse number M for PWM (red) and PWC (blue) at $t = 100\mu s$ under different Hamiltonians, where noise amplitude $1 \times 10^{-3}\mu s$.

V. ROBUSTNESS ANALYSIS

To combine PWM with experimental quantum simulation, we further test the performance of PWM with noises on the pulse width t_p to mimic the experimental condition with imperfect switch. For example, the evolution operator with switching noise δ calculated by PWC and PWM, can be respectively present as

$$\hat{U}(t+\tau,t) = \exp\Big[-i(\tau+\delta)(H_0 + u(t+\frac{\tau}{2})\hat{H}_1)\Big] \leftrightarrow$$
$$\hat{U}_M(t+\tau,t) = \exp\Big[-i(t_f - \frac{\delta}{2})\hat{H}_0\Big]$$
$$\times \exp\Big[-i(t_p+\delta)(H_0 \pm \xi\hat{H}_1)\Big]\exp\Big[-i(t_f-\frac{\delta}{2})\hat{H}_0\Big],$$

where the term $(t_f - \frac{\delta}{2})$ comes from the equality $t_f + t_p \equiv \tau$. From this point of view, we may expect the influence of noise in term $\exp[-i(t_f - \frac{\delta}{2})\hat{H}_0]$ will counteract partial that of the noise in $\exp[-i(t_p+\delta)(H_0 \pm \xi\hat{H}_1)]$, and thus make PWM more robust for possible noises and more applicable in laboratory.

Figures 4(a) and (b) show the relation between error ε under switching noise and pulse number M for both PWM and PWC for different number of controls $u_k(t)$, respectively. For a relatively small M, PWC is slightly more accurate than PWM; as M gets larger and larger, this advantage becomes more and more negligible, but the influence of switching noise becomes more and more conspicuous; nevertheless, PWM always shows a much more robust performance than PWC. Though somewhat counter intuitive, numerical results show that the unremitting on and off pulses, i.e. the PWM pulses, is less sensitive to the switching noises in potential experimental realization. Though PWC has been broadly accepted in experiments (e.g. experimental quantum simulation[4]), our study suggests that PWM is a even better choice to accomplish delicate controls in laboratory.

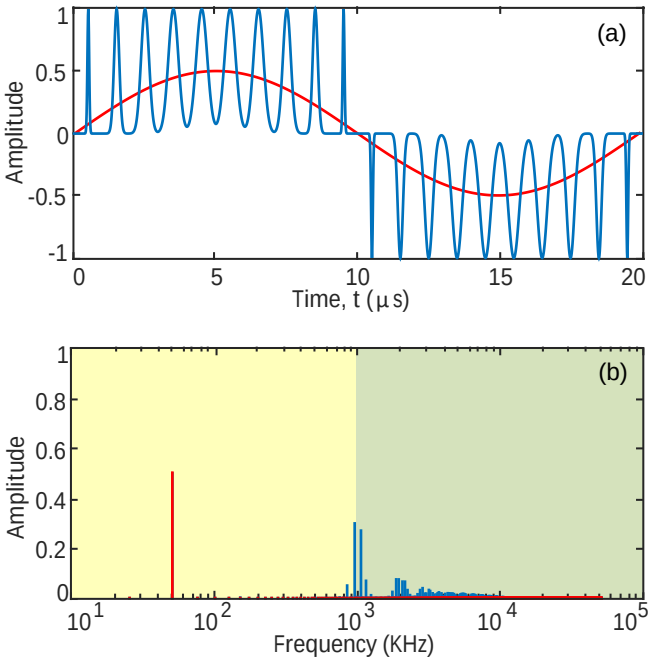

FIG. 5. (Color online) Schematic for PWM transformation. (a), (b) Time-dependent function $1/2\sin\omega t$ of frequency $\omega = 50$KHz (red) and the corresponding 20-step Gaussian PWM form (blue) in time domain and in frequency domain, respectively. The areas within and without the frequency scope $\Omega = 1$MHz are distinguished by yellow and green color, respectively.

VI. OTHER REALIZATIONS OF PWM TRANSFORMATION

Based on EAP, one can develop various realizations of PWM transformation. Besides the strategy that simultaneously raising the pulse amplitude ξ and shrink the pulse duration t_p by the same factor, we can also transform the Hamiltonian into other forms, for example

$$\{\hat{H}_0 + u(t)\hat{H}_1\} \leftrightarrow \{\hat{H}_0 \pm \xi\hat{H}_1\},$$

or use other functions to replace the rectangular pulses. These various realizations may facilitate specific applications to experimental quantum simulations, e.g. shaped femtosecond pulses in laser control systems[44]. For demonstration, we transform the rectangular PWM pulses into Gaussian pulses as fellows.

Suppose there is a superposition of M Gaussian pulse trains with identical period $T = 2\pi/\omega_{min}$ and amplitude ξ, but different parameter $t_{p,k}^{(m)}$ and pulse center $(m-\frac{1}{2})\tau$ for $\tau = T/M$, it can be Fourier expanded as

$$\tilde{u}_k(t) = \sum_{n=-\infty}^{+\infty}\Big(\frac{\xi}{T}\sum_{m=1}^{M} t_{p,k}^{(m)} e^{-\frac{(n\omega_{min}t_p^{(m)})^2}{4\pi}} \times e^{-in\omega_{min}(m-\frac{1}{2})\tau}\Big)e^{in\omega_{min}t}. \quad (7)$$

A simple approximation shows

$$\frac{\xi}{T}\sum_{m=1}^{M} t_{p,k}^{(m)} e^{-\frac{(n\omega_{min}t_{p,k}^{(m)})^2}{4\pi}} \approx \frac{\xi t_{p,k}^{(m)}}{M\tau},$$

thus Eq. (7) can be approximated as

$$\tilde{u}_k(t) = \sum_{n=-\infty}^{+\infty}\left(\sum_{m=1}^{M}\frac{\xi t_{p,k}^{(m)}}{M\tau}e^{-in\omega_{min}(m-\frac{1}{2})\tau}\right)e^{in\omega_{min}t}. \tag{8}$$

When choosing

$$t_{p,k}^{(m)} = \xi^{-1}\int_{m\tau}^{(m+1)\tau} dt' u_k(t'),$$

Eq. (8) becomes exactly the same as that obtained for the rectangular pulses Eq. (4). Thus, the rectangular pulses can be well replaced by Gaussian pulses under the same definition of $t_{p,k}^{(m)}$. On the other hand, it facilitates us to use the rectangular PWM form for simulating quantum dynamics for saving CPU time, and directly transform the results into Gaussian pulses (or other convenient forms) for experimental realization for implementing robust control.

Figure 5(a) shows the relation between the original function $1/2\sin(\omega t)$ and the corresponding Gaussian PWM pulses in time domain, Fig. 5(b) reveals the properties of the twos in frequency domain. Consistent with our former analysis, these Gaussian pulses can exactly pick all frequency terms of the original function $u(t)$ within the scope $\Omega = M\omega_{min}$, with very small noise only outside Ω. This demonstrates the PWM transformation can be realized by various forms by using EAP, and thus may be very applicable in specific experiments.

VII. CONCLUSIONS

In summary, we presented a Pulse Width Modulation (PWM) approach for simulating quantum dynamics with finite spectral bandwidth by transforming an arbitrary time-dependent Hamiltonian into a sequence of time-independent ones. Numerical tests show that PWM can outperform the standard piecewise-constant (PWC) approximation and the SPO approximation in accelerating computational quantum simulation at high precision within $N \leq 10$ qubit systems. In addition, PWM is also more robust to the switching noise and can be realized in various forms, e.g. Gaussian pulse train. Therefore, PWM method provides new ways for simulating which may be further applied to design more efficient control strategies for optimizing time-dependent quantum dynamics. This will be studied in our future work.

ACKNOWLEDGEMENTS

This work is supported by the National Natural Science Foundation of China (Grants No. 61134008, No. 61374091, and No. 91221205). We thank Professor Herschel Rabitz from Princeton University for useful discussions.

Appendix A: The derivation of PWM

We define the Frequency Band $\Delta \equiv [\omega_{min}, \omega_{max}]$ as the interval from the minimum to the maximum frequency of all the time-dependent variables in the Hamiltonian. Consider an arbitrary time-dependent Hamiltonian in the semiclassical form

$$\hat{H}(t) = \hat{H}_0 + \sum_{k=1}^{K} u_k(t)\hat{H}_k, \tag{A1}$$

where H_0 and H_k are time-independent Hamiltonians, $u_k(t)$'s are time-dependent real functions. After applying Fourier Transformation on $u_k(t)$, we obtain

$$\mathcal{U}_k(\omega) = \int_{-\infty}^{+\infty} dt e^{-i\omega t}u_k(t),$$
$$\mathcal{U}_k^*(\omega) = \mathcal{U}_k(-\omega);$$

we then apply anti-Fourier Transition on both sides and transform $\mathcal{U}_k(\omega)$ back to the time domain

$$u_k(t) = \frac{1}{\pi}\int_{\omega_{min}}^{\omega_{max}} d\omega A_{\omega,k}\sin(\omega t + \phi_k(\omega)). \tag{A2}$$

where

$$A_k(\omega) = |\mathcal{U}_k(\omega)|,\ k = 1, \cdots, K;$$
$$\phi_k(\omega) = \pi - \arg\{\mathcal{U}_k(\omega)\},\ k = 1, \cdots, K.$$

The reason for doing this is to express the functions $u_k(t)$ by a superposition of sinusoidal functions, in other words

$$\hat{H}(t) = \hat{H}_0 + \frac{1}{\pi}\sum_{k=1}^{K}\int_{\omega_{min}}^{\omega_{max}} d\omega A_k(\omega)\sin(\omega t + \phi_k(\omega))\hat{H}_k.$$

For example, when $u_k(t)$ is periodic or multi-periodic, we get

$$\hat{H}(t) = \frac{1}{2}\sum_{k=0}^{K} A_{0,k}\hat{H}_k + \sum_{n=1}^{N}\sum_{k=1}^{K} A_{n,k}\sin(n\omega_k t + \phi_{n,k})\hat{H}_k,$$

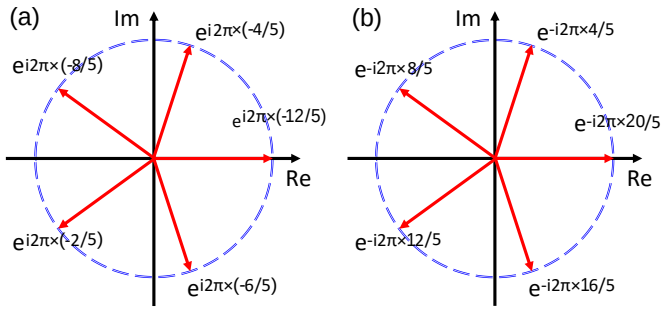

FIG. 6. (Color online) (a), (b) Schematic for cancellation of the two summations $\sum_{m=1}^{M} e^{i\frac{(1-n)m}{M}2\pi} = 0$ as well as $\sum_{m=1}^{M} e^{-i\frac{(1+n)m}{M}2\pi} = 0$ for $M = 5$, $n = 3$.

where

$$A_{0,0} = 2,\ A_{0,k} = \frac{\omega_k}{\pi}\int_0^{2\pi/\omega_k} dt u_k(t);$$
$$A_{n,k} = \frac{\omega_k}{\pi}\Big\{\Big[\int_0^{2\pi/\omega_k} dt u_k(t)\cos(n\omega_k t)\Big]^2 + \Big[\int_0^{2\pi/\omega_k} dt u_k(t)\sin(n\omega_k t)\Big]^2\Big\}^{\frac{1}{2}};$$
$$\tan(\phi_{n,k}) = \frac{\int_0^{2\pi/\omega_k} dt u_k(t)\cos(n\omega_k t)}{\int_0^{2\pi/\omega_k} dt u_k(t)\sin(n\omega_k t)}.$$

Our aim is to change the original time-dependent Hamiltonian into "Hamiltonian Pulses", and accordingly we can achieve this by transforming all the sinusoidal functions into pulses. We first consider the simplest Hamiltonian of the form

$$\hat{H}(t) = \hat{H}_0 + \sin(\omega t + \phi)H_1,$$

where the sinusoidal function can be written as

$$\sin(\omega t + \phi) = -\frac{e^{-i\phi}}{2i}e^{-i\omega t} + \frac{e^{i\phi}}{2i}e^{i\omega t}. \tag{A3}$$

For a periodic pulse function $f(t)$ centered at $t = 0$, with period $T = 2\pi/\omega$, amplitude ξ, and pulse width t_p, it can be Fourier expanded as

$$f(t) = \frac{\omega}{2\pi}\xi t_p + \sum_{n=-\infty, n\neq 0}^{+\infty}\frac{\xi}{n\pi}\sin\Big(\frac{n\omega}{2}t_p\Big)e^{in\omega t}.$$

Suppose there is a superposition of M rectangular functions $f_m(t)$ centered at $(m-1/2)\tau$ for $\tau = T/M$, with the same period $T = 2\pi/\omega$ and amplitude ξ but different pulse width $t_p^{(m)}$, it can be Fourier expanded as

$$\sum_{m=1}^{M} f_m(t) = \frac{\xi}{T}\sum_{m=1}^{M} t_p^{(m)} + \sum_{n=-\infty, n\neq 0}^{+\infty}\Big[\sum_{m=1}^{M}\frac{\xi}{n\pi}\sin\Big(\frac{t_p^{(m)}}{\tau}\frac{n\pi}{M}\Big)e^{-in\omega(m-\frac{1}{2})\tau}\Big]e^{in\omega t}. \tag{A4}$$

Compare Eq. (A3) with Eq. (A4), one should choose the parameter M and $t_p^{(m)}$ as

$$\frac{\xi}{T}\sum_{m=1}^{M} t_p^{(m)} = 0, \tag{A5}$$
$$\sum_{m=1}^{M}\frac{\xi}{n\pi}\sin\Big(\frac{t_p^{(m)}}{\tau}\frac{n\pi}{M}\Big)e^{-in\omega(m-\frac{1}{2})\tau} = -\frac{e^{-i\phi}}{2i}\delta_{-1,n} + \frac{e^{i\phi}}{2i}\delta_{1,n}, \tag{A6}$$

where $\delta_{1,n}$ is the Kronecker Delta function. However, a more detailed calculation shows that this condition cannot be exactly satisfied by a superposition of finite rectangular functions; to approximately satisfy the condition, we define

$$t_p^{(m)} = \frac{1}{\xi}\int_{m\tau}^{(m+1)\tau} dt'\sin(\omega t' + \phi) = \frac{1}{2\xi\omega}\Big(e^{i\phi}e^{i\omega m\tau} - e^{i\phi}e^{i\omega(m+1)\tau} + c.c\Big).$$

Suppose $M \gg n$, a simple approximation gives that

$$\sum_{m=1}^{M}\frac{\xi}{n\pi}\sin\Big(\frac{t_p^{(m)}}{\tau}\cdot\frac{n\pi}{M}\Big) \approx \sum_{m=1}^{M}\frac{\xi t_p^{(m)}}{M\tau},\ n \ll M.$$

When $M \gg n$ is not satisfied, the approximation is also reasonable since the corresponding frequency is very high and the coefficient $1/n$ is very small. The idea is very similar to the Rotating Wave Approximation (RWA), where we suppose the terms with higher frequency than ω_{min} with small coefficients contribute very little to the dynamics of the system. A more detailed calculation shows that

$$\sum_{m=1}^{M}\frac{\xi}{n\pi}\sin\Big(\frac{t_p^{(m)}}{\tau}\frac{n\pi}{M}\Big)e^{-in\omega(m-\frac{1}{2})\tau} = \frac{e^{in\omega\tau/2}}{4\pi}\Big[\Big(1-e^{i\omega\tau}\Big)e^{i\phi}\sum_{m=1}^{M}e^{im\omega\tau(1-n)} + \Big(1-e^{-i\omega\tau}\Big)e^{-i\phi}\sum_{m=1}^{M}e^{-im\omega\tau(1+n)}\Big], \tag{A7}$$

for $n = 1$,

$$\frac{\xi}{M}\sum_{m=1}^{M}\frac{t_p^{(m)}}{\tau}e^{-i\omega(m-\frac{1}{2})\tau} = \frac{e^{i\frac{\pi}{M}}}{4\pi}\Big[M\Big(1-e^{i\frac{2\pi}{M}}\Big)e^{i\phi} + \Big(1-e^{-i\frac{2\pi}{M}}\Big)e^{-i\phi}\sum_{m=1}^{M}e^{-i\frac{2m}{M}2\pi}\Big] \simeq \frac{e^{i\phi}}{2i};$$

for $n = -1$,

$$\frac{\xi}{M}\sum_{m=1}^{M}\frac{t_p^{(m)}}{\tau}e^{i\omega(m-\frac{1}{2})\tau} = \frac{e^{-i\frac{\pi}{M}}}{4\pi}\Big[\Big(1-e^{i\frac{2\pi}{M}}\Big)e^{i\phi}\sum_{m=1}^{M}e^{i\frac{2m}{M}2\pi} + M\Big(1-e^{-i\frac{2\pi}{M}}\Big)e^{-i\phi}\Big] \simeq -\frac{e^{-i\phi}}{2i};$$

for $n \neq \pm 1$, the result is not so obvious; however, as long as $|n| \neq lM \pm 1,\ l = 1, 2, \cdots$, one can derive that

$$\begin{aligned}
&\frac{\xi}{M}\sum_{m=1}^{M}\frac{t_p^{(m)}}{\tau}e^{-in\omega(m-\frac{1}{2})\tau} \\
&= \frac{e^{in\frac{\pi}{M}}}{4\pi}\Big[\Big(1-e^{i\frac{2\pi}{M}}\Big)e^{i\phi}\sum_{m=1}^{M}e^{i\frac{(1-n)m}{M}2\pi} \\
&\quad + \Big(1-e^{-i\frac{2\pi}{M}}\Big)e^{-i\phi}\sum_{m=1}^{M}e^{-i\frac{(1+n)m}{M}2\pi}\Big] = 0.
\end{aligned}$$

Figure 6 illustrates how the two summations annihilate when $M = 5$, $n = 3$. The approach of deriving PWM transformation of a single period function $\sin(\omega t + \phi)$ reveals that the superposition of M pulses have exactly the same components in frequency domain within $M\omega$, with difference only outside $M\omega$. Thus, we call $\Omega = M\omega$ the Frequency Scope which is a very important concept which index the frequency limit within which we can satisfy Eq. (A5) and (A6) by properly choosing pulse width $t_p^{(m)}$, called the M-step PWM pulses.

Next, we consider a more complex Hamiltonian

$$\hat{H}(t) = \hat{H}_0 + u(t)H_1.$$

Since $u(t)$ is a superposition of sinusoidal functions according to Eq. (A2), we can always properly choose the pulse amplitudes for each frequency component ω and generate PWM pulse with the same width $t_p^{(m)}$

$$t_p^{(m)} = \frac{A(\omega)}{\xi(\omega)}\int_{m\tau}^{(m+1)\tau} dt' \sin(\omega t' + \phi(\omega)),$$

where $\tau = 2\pi/M\omega_{min}$. Moreover, if we further request

$$\frac{1}{\pi}\int_{\omega_{min}}^{\omega_{max}} d\omega\xi(\omega) = \xi,$$

where ξ is a constant, thus we obtain

$$\xi = \frac{1}{t_p^{(m)}}\int_{m\tau}^{(m+1)\tau} dt' \int_{\omega_{min}}^{\omega_{max}} d\omega A(\omega)\sin(\omega t' + \phi_(\omega)),$$

and accordingly

$$t_p^{(m)} = \xi^{-1}\int_{m\tau}^{(m+1)\tau} dt' u(t').$$

Based on this, we can derive a very useful principle for designing PWM pulses without redo Fourier transformation, called the *Equal Integral Area Principle* (EAP):

When designing M-step PWM transformation for the Hamiltonian of Eq. (A1), we divide every time interval $2\pi/\omega_{min}$ into M pieces with equal length τ, in each we replace $u_k(t)$ by a rectangular function with amplitude ξ and width t_p which contains the same integral area.

By transfering every functions $u_k(t)$ into rectangular pulses, we finally comes to the general Hamiltonian as described in Eq. (A1)

$$\hat{H}(t) = \hat{H}_0 + \sum_{k=1}^{K} u_k(t)\hat{H}_k,$$

and transform the time-dependent Hamiltonian into the piecewise time-independent form, saying the PWM form

$$\hat{H}(t) = \hat{H}_0 + \sum_{k} s_k(t)\xi_k\hat{H}_k,$$

where$s_{t,k} = 0, \pm 1$ is a sign function can be regarded as a sequence of unitary pulses with time, and the default pulse amplitude $\xi_k = \max_t |u_k(t)|$ if without further declaration.

Appendix B: The priori error formula

According to the Schrödinger Equation (SE) of the general time-dependent Hamiltonian $\hat{H}(t)$ and the piecewise time-independent Hamiltonian $\hat{H}_M(t)$ transformed by the M-step PWM transformation, we obtain two time evolutions of the corresponding two propagators

$$\begin{aligned}
i\frac{\partial}{\partial t}\hat{U}(t) &= \hat{H}(t)\hat{U}(t), \\
i\frac{\partial}{\partial t}\hat{U}_M(t) &= \hat{H}_M(t)\hat{U}_M(t),
\end{aligned}$$

where footnote M represents it is calculated by M-step PWM transformation. To evaluate the difference of the two propagators, we define Error Operator $\hat{E}(t) = \hat{U}(t) - \hat{U}_M(t)$ with $\hat{E}(0) = 0$, and obtain the dynamics of $\hat{E}(t)$

$$\begin{aligned}
\frac{\partial}{\partial t}\hat{E}(t) &= -i\left(\hat{H}(t)\hat{U}(t) - \hat{H}_M(t)\hat{U}_M(t)\right) \qquad \text{(B1)} \\
&= -i\hat{H}(t)\hat{E}(t) - i\left(\hat{H}(t) - \hat{H}_M(t)\right)\hat{U}_M(t).
\end{aligned}$$

Since $\hat{E}(t)$ and $\hat{U}_M(t)$ are independent time-dependent functions, Eq. (B1) is exactly of the form of the standard time-varying linear system in Linear System Theory[45], that is

$$\frac{\partial}{\partial t}\hat{x}(t) = \hat{A}(t)\hat{x}(t) + \hat{B}(t)\hat{u}(t),$$

which have the formal solution

$$\hat{x}(t) = \hat{\Phi}(t,0)\hat{x}_0 + \int_0^t dt'\hat{\Phi}(t,t')\hat{B}(t')\hat{u}(t'), \quad \text{(B2)}$$

$$\begin{aligned}
\hat{\Phi}(t,t_0) &= \hat{I} + \int_{t_0}^{t} dt'\hat{A}(t') \\
&\quad + \int_{t_0}^{t}\int_{t_0}^{t_1'} dt_1' dt_2'\hat{A}(t_1')\hat{A}(t_2') + \cdots, \qquad \text{(B3)}
\end{aligned}$$

where $\hat{x}(t)$ is called the "state", $\hat{u}(t)$ is called the "control", $\Phi(t,t_0)$ is called the "state transition matrix". Put Eq. (B1) into Eq. (B2) and (B3), we obtain the formula of the error operator

$$\hat{E}(t) = -i\int_0^t dt'\hat{U}(t,t')\left(\hat{H}(t') - \hat{H}_M(t')\right)\hat{U}_M(t'), \tag{B4}$$

where

$$\begin{aligned}\hat{U}(t,t_0) = \hat{I} + (-i)\int_{t_0}^t dt'\hat{H}(t') \\ +(-i)^2\int_{t_0}^t\int_{t_0}^{t_1'} dt_1'dt_2'\hat{H}(t_1')\hat{H}(t_2') + \cdots\end{aligned}$$

is exactly the Dyson Series of the evolution operator from time t_0 to t.

To further provide a quantitative result of $\hat{E}(t)$, we define the complex error function ε

$$\varepsilon(t) = \frac{1}{2}\Big|\langle\psi(t)|\hat{\Gamma}(t)|\psi_0\rangle\Big| = \frac{1}{2}\Big|1 - \langle\psi(t)|\hat{U}_M(t)|\psi_0\rangle\Big|,$$

which describes the error of the two propagators at time t, where the factor $1/2$ is for normalization. Associate with Eq. (B4), we obtain

$$\varepsilon(t) \simeq \frac{1}{2}\Big|\int_0^t dt'\langle\psi(t')|\Big(\hat{H}_M(t') - \hat{H}(t')\Big)|\psi(t')\rangle\Big|,$$

where the approximation lies in the approximation $|\psi(t')\rangle \simeq U_M(t')|\psi_0\rangle$ since we suppose $U(t')$ and $U_M(t')$ do not vary too much. To distinguish from the accurate error ε, we name it the Priori Error ε_p to make an estimation of the actual error ε.

We first consider the Hamiltonian contains only one sinusoidal function

$$\hat{H}(t) = \hat{H}_0 + \sin(\omega t + \phi)\hat{H}_1.$$

where $\hat{H}_0$ and $\hat{H}_1$ are time-independent Hamiltonians. According to the result Eq. (A4) and (A7), we obtain the difference between of the original time-dependent Hamiltonian $\hat{H}(t)$ and the piecewise time-independent Hamiltonian $\hat{H}_M(t)$ transformed by the M-step PWM transformation

$$\begin{aligned}&\hat{H}_M(t') - \hat{H}(t') \\ &= \hat{H}_1\frac{M}{\pi}\left[\cos\Big((\omega t+\phi) + \frac{\pi}{M}\Big) - \cos\Big((\omega t+\phi) + \frac{3\pi}{M}\Big)\right] \\ &\quad\times\sum_{l=1}^{\infty}\cos\Big(lM(\omega t+\phi) + l\pi\Big) \\ &= \hat{H}_1 2\sqrt{2}\cos\Big((\omega t+\phi) + \frac{\pi}{4}\Big)\sum_{l=1}^{\infty}(-1)^l\cos\Big(lM(\omega t+\phi)\Big).\end{aligned}$$

Thus

$$\begin{aligned}\varepsilon_p(t) = \sqrt{2}\Big|\int_0^t dt'\langle\psi_0|\hat{H}_1(t')|\psi_0\rangle\cos\Big((\omega t'+\phi) + \frac{\pi}{4}\Big) \\ \times\sum_{l=1}^{\infty}(-1)^l\cos\Big(lM(\omega t'+\phi)\Big)\Big|.\end{aligned}$$

where $\hat{H}_1(t') = \hat{U}^\dagger(t')\hat{H}_1\hat{U}(t')$.

Following the same procedure in App. A, we finally obtain the priori error formula for the Hamiltonian of Eq. (A1) by integrating Eq. (B5) over $\omega \in \Delta$ and summarising k

$$\varepsilon_p(t) = \frac{\sqrt{2}}{\pi}\Big|\sum_{k=1}^{K}\int_{\omega_{min}}^{\omega_{max}} d\omega\int_0^t dt'\langle\psi_0|\hat{H}_k(t')|\psi_0\rangle\cos\Big(\omega t' + (\phi_k(\omega) + \frac{\pi}{4})\Big)\sum_{l=1}^{\infty}(-1)^l\cos\Big(lM(\omega t'+\phi)\Big)\Big|.$$

[1] L. M. K. Vandersypen and I. L. Chuang, "Nmr techniques for quantum control and computation," Rev. Mod. Phys. **76**, 1037–1069 (2005).

[2] J. J. Sakurai and S. F. Tuan, *Modern Quantum Mechanics* (Addison-Wesley, 1994).

[3] Y. Wu and X. Yang, "Strong-coupling theory of periodically driven two-level systems," Phys. Rev. Lett. **98**, 013601 (2007).

[4] I. M. Georgescu, S. Ashhab, and F. Nori, "Quantum simulation," Rev. Mod. Phys. **86**, 153–185 (2014).

[5] H. F. Trotter, "On the product of semi-groups of operators," Proc. Amer. Math. Soc. **10**, 545–551 (1959).

[6] K. R. Brown, R. J. Clark, and I. L. Chuang, "Limitations of quantum simulation examined by simulating a pairing hamiltonian using nuclear magnetic resonance," Phys. Rev. Lett. **97**, 050504 (2006).

[7] C. R. Clark, T. S. Metodi, S. D. Gasster, and K. R. Brown, "Resource requirements for fault-tolerant quantum simulation: The ground state of the transverse ising model," Phys. Rev. A **79**, 062314 (2009).

[8] H. Weimer, M. Müller, H. P. Büchler, and I. Lesanovsky, "Digital quantum simulation with rydberg atoms," Quantum Information Processing **10**, 885–906 (2011).

[9] C. Weitenberg, M. Endres, J. F. Sherson, M. Cheneau, P. Schauß, T. Fukuhara, I. Bloch, and S. Kuhr, "Single-spin addressing in an atomic mott insulator," Nature **471**, 319–324 (2011).

[10] D. Poulin, A. Qarry, R. Somma, and F. Verstraete, "Quantum simulation of time-dependent hamiltonians and the convenient illusion of hilbert space," Phys. Rev. Lett. **106**, 170501 (2011).

[11] S. Somaroo, C. H. Tseng, T. F. Havel, R. Laflamme, and D. G. Cory, "Quantum simulations on a quantum computer," Phys. Rev. Lett. **82**, 5381–5384 (1999).

[12] L. Lamata, J. León, T. Schätz, and E. Solano, "Dirac equation and quantum relativistic effects in a single trapped ion," Phys. Rev. Lett. **98**, 253005 (2007).

[13]R. Gerritsma, G. Kirchmair, F. Zähringer, E. Solano, R. Blatt, and C. Roos, "Quantum simulation of the dirac equation," Nature **463**, 68–71 (2010); R. Gerritsma, B. P. Lanyon, G. Kirchmair, F. Zähringer, C. Hempel, J. Casanova, J. J. García-Ripoll, E. Solano, R. Blatt, and C. F. Roos, "Quantum simulation of the klein paradox with trapped ions," Phys. Rev. Lett. **106**, 060503 (2011).

[14]J. I. Cirac and F. Verstraete, "Renormalization and tensor product states in spin chains and lattices," Journal of Physics A: Mathematical and Theoretical **42**, 504004 (2009).

[15]K. Temme, T. Osborne, K. G. Vollbrecht, D. Poulin, and F. Verstraete, "Quantum metropolis sampling," Nature **471**, 87–90 (2011) is immune to the sign problem in Monte Carlo method.

[16]E. T. Jaynes and F. W. Cummings, "Comparison of quantum and semiclassical radiation theories with application to the beam maser," Proceedings of the IEEE **51**, 89–109 (1963).

[17]M. Srinivas and E. Davies, "Photon counting probabilities in quantum optics," Optica Acta **28**, 981–996 (1981).

[18]J. C. A. Barata and W. F. Wreszinski, "Strong-coupling theory of two-level atoms in periodic fields," Phys. Rev. Lett. **84**, 2112–2115 (2000).

[19]E. K. Irish, J. Gea-Banacloche, I. Martin, and K. C. Schwab, "Dynamics of a two-level system strongly coupled to a high-frequency quantum oscillator," Phys. Rev. B **72**, 195410 (2005).

[20]I. Guedes, "Solution of the schrödinger equation for the time-dependent linear potential," Phys. Rev. A **63**, 034102 (2001).

[21]H. Bekkar, F. Benamira, and M. Maamache, "Comment on "solution of the schrodinger equation for the time-dependent linear potential"," Phys. Rev. A **68**, 016101 (2003).

[22]P. G. Luan and C. S. Tang, "Lewis-riesenfeld approach to the solutions of the schrödinger equation in the presence of a time-dependent linear potential," Phys. Rev. A **71**, 014101 (2005).

[23]M. Feng, "Complete solution of the schrödinger equation for the time-dependent linear potential," Phys. Rev. A **64**, 034101 (2001).

[24]A. Palma, M. Villa, and L. Sandoval, "On the time-dependent solutions of the schrodinger equation. i. the linear time-dependent potential," International Journal of Quantum Chemistry **111**, 1646–1650 (2011).

[25]R. Jackiw and S.-Y. Pi, "Soliton solutions to the gauged nonlinear schrödinger equation on the plane," Phys. Rev. Lett. **64**, 2969–2972 (1990).

[26]J. H. Shirley, "Solution of the schrödinger equation with a hamiltonian periodic in time," Phys. Rev. **138**, B979–B987 (1965).

[27]T. Levante, M. Baldus, B. Meier, and R. Ernst, "Formalized quantum mechanical floquet theory and its application to sample spinning in nuclear magnetic resonance," Molecular Physics **86**, 1195–1212 (1995).

[28]U. Haeberlen and J. S. Waugh, "Coherent averaging effects in magnetic resonance," Phys. Rev. **175**, 453–467 (1968).

[29]E. S. Mananga and T. Charpentier, "Introduction of the floquet-magnus expansion in solid-state nuclear magnetic resonance spectroscopy," The Journal of Chemical Physics **135**, 044109 (2011).

[30]R. Kosloff, "Time-dependent quantum-mechanical methods for molecular dynamics," J.Phys. Chem. **92**, 2087–2100 (1988).

[31]A. Castro, M. A. L. Marques, and A. Rubio, "Propagators for the time-dependent kohnsham equations," The Journal of Chemical Physics **121**, 3425–3433 (2004).

[32]A. Askar and A. S. Cakmak, "Explicit integration method for the timedependent schrodinger equation for collision problems," J. Chem. Phys. **68**, 2794–2798 (1978).

[33]D. Kosloff and R. Kosloff, "A fourier method solution for the time dependent schrdinger equation as a tool in molecular dynamics," J. Comput. Phys. **52**, 35 – 53 (1983).

[34]H. Tal-Ezer and R. Kosloff, "An accurate and efficient scheme for propagating the time dependent schrdinger equation," J. Chem. Phys. **81**, 3967–3971 (1984).

[35]M. Ndong, H. Tal-Ezer, R. Kosloff, and C. P. Koch, "A chebychev propagator with iterative time ordering for explicitly time-dependent hamiltonians," The Journal of chemical physics **132**, 064105 (2010).

[36]C. Leforestier, R. Bisseling, C. Cerjan, M. Feit, R. Friesner, A. Guldberg, A. Hammerich, G. Jolicard, W. Karrlein, H.-D. Meyer, N. Lipkin, O. Roncero, and R. Kosloff, "A comparison of different propagation schemes for the time dependent schrodinger equation," J. Comput. Phys. **94**, 59 – 80 (1991).

[37]J. Fleck, J. J. Morris, and M. Feit, "Time-dependent propagation of high energy laser beams through the atmosphere," Appl. Phys. **10**, 129 – 160 (1976).

[38]M. Feit, J. Fleck, and A. Steiger, "Solution of the schrodinger equation by a spectral method," J. Comput. Phys. **47**, 412 – 433 (1982); M. D. Feit and J. A. Fleck, "Solution of the schrdinger equation by a spectral method ii: Vibrational energy levels of triatomic molecules," The Journal of Chemical Physics **78**, 301–308 (1983).

[39]M. Suzuki, "Quantum statistical monte carlo methods and applications to spin systems," Journal of Statistical Physics **43**, 883–909 (1986); "Fractal decomposition of exponential operators with applications to many-body theories and monte carlo simulations," Physics Letters A **146**, 319 – 323 (1990).

[40]A. D. Bandrauk and H. Shen, "Higher order exponential split operator method for solving time-dependent schrodinger equations," Can. J. Chem. **70**, 555–559 (1992); "Exponential split operator methods for solving coupled time-dependent schrodinger equations," The Journal of Chemical Physics **99**, 1185–1193 (1993).

[41]D. G. Holmes and T. A. Lipo, *Pulse width modulation for power converters: principles and practice*, Vol. 18 (Wiley-IEEE Press, 2003).

[42]F. Vasca and L. Iannelli, *Dynamics and Control of Switched Electronic Systems* (Springer London, 2012) pp. 25-61

[43]The CPU time t_c is measured using the *tic* and *toc* commands in *Matlab* 2014*b*.

[44]A. Assion, T. Baumert, M. Bergt, T. Brixner, B. Kiefer, V. Seyfried, M. Strehle, and G. Gerber, "Control of chemical reactions by feedback-optimized phase-shaped femtosecond laser pulses," Science **282**, 919–922 (1998).

[45]D. Zheng, *Linear System Theory* (Tsinghua University Press, 2002).

[46]T. M. Zhang, R. B. Wu, F. H. Zhang, T. J. Tarn, and G. L. Long, "Minimum-time selective control of homonuclear spins," IEEE Transactions on Control Systems Technology **23**, 2018–2025 (2015).

[47]Q. M. Chen, R. B. Wu, T. M. Zhang, and H. Rabitz, "Near-time-optimal control for quantum systems," Phys. Rev. A **92**, 063415 (2015).

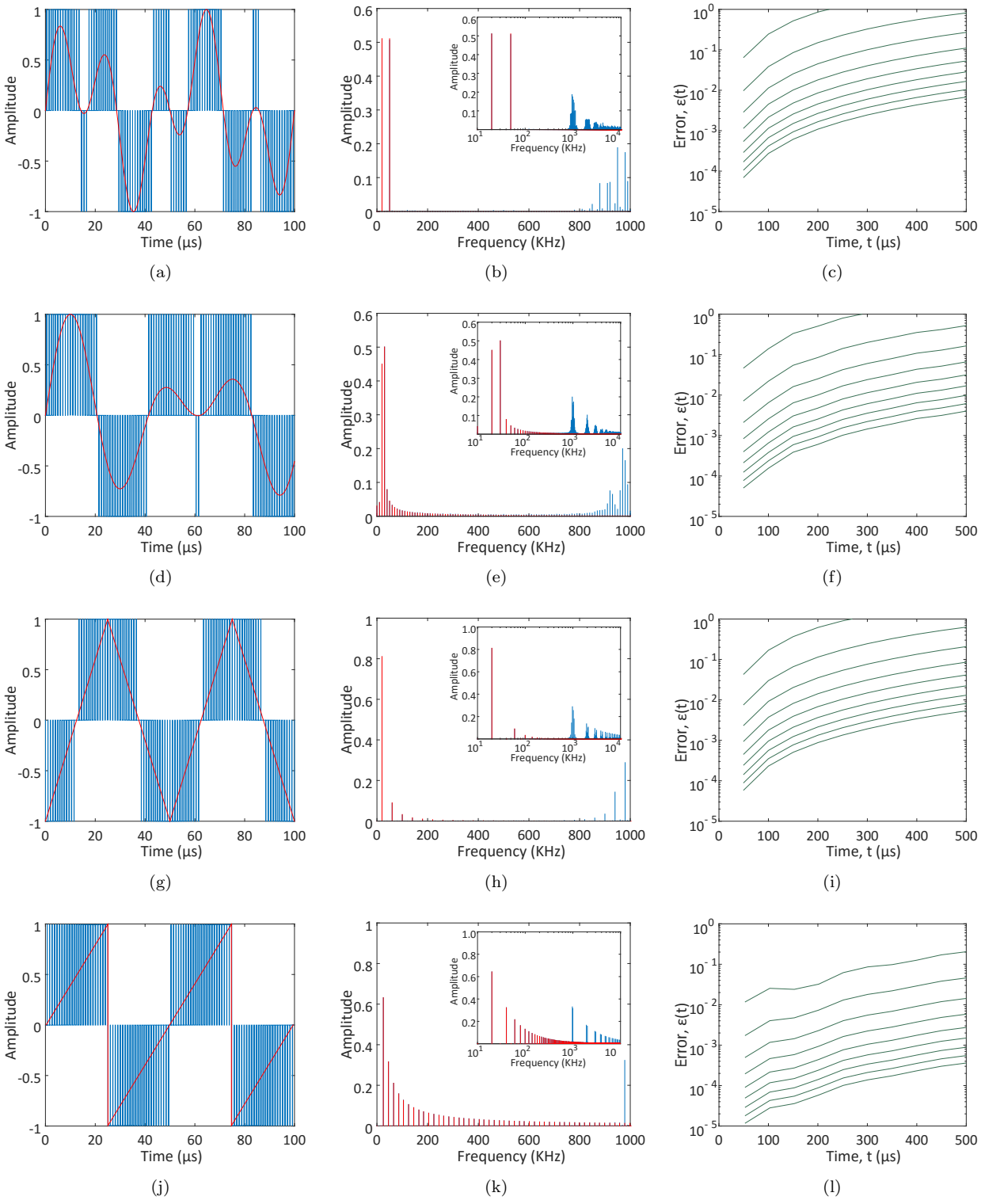

FIG. 7. (Color online) Time-dependent function (red) and the corresponding PWM form with $\Omega = 1$MHz (blue) in time domain and in frequency domain, where the inset show detailed properties in frequency domain within a larger range. (a), (b) $1/N\left(\sin\left(\omega_1 t\right) + \sin\left(\omega_2 t\right)\right)$, where N is the normalization number, with $\omega_1 = 20$KHz, $\omega_2 = 50$KHz; (d), (e) with $\omega_1 = 20$KHz, $\omega_2 = 20\sqrt{2}$KHz; (g), (h) periodic triangular wave function with frequency 20KHz; (j), (k) sawtooth wave function with frequency 20KHz. (c), (f), (i), (l) show dependence of error ε on evolution time t for PWM transformation on these different function, where each line corresponds to a different pulse number $M = 20, \cdots, 100$ from top to the bottom.

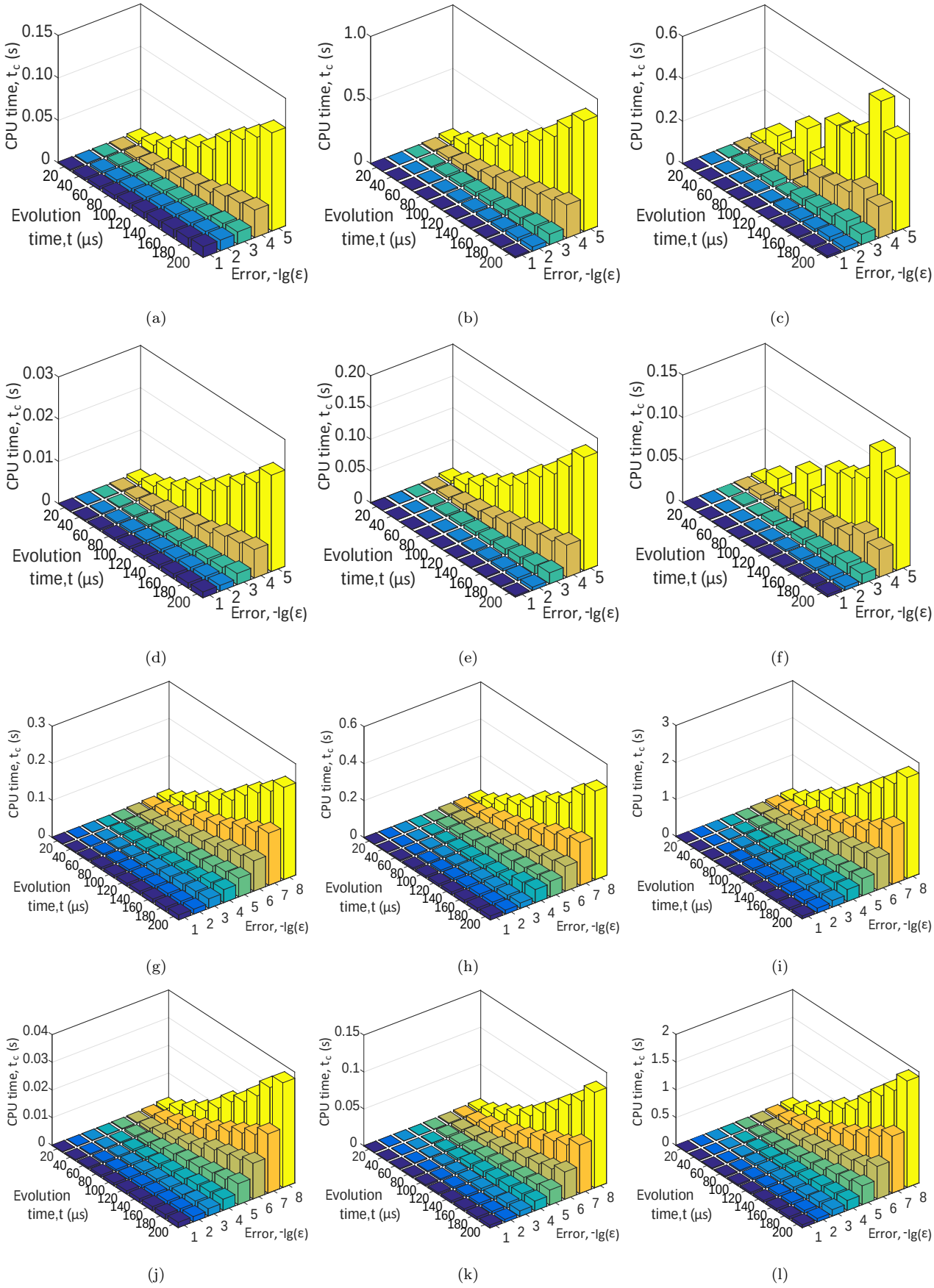

FIG. 8. (Color online) CPU time t_c with evolution time t and accuracy requirement ε for PWC and PWM. (a), (d) 2-dimensional case in weak-coupling regime $\kappa_1 = 0.1$; (b), (e) 2-dimensional case in moderate-coupling regime $\kappa_1 = 1$; (c), (f) 2-dimensional case in strong-coupling regime $\kappa_1 = 10$; (g), (j) 4-dimensional case with $\kappa_1 = 1$; (h), (k) 16-dimensional case with $\kappa_1 = 1$; (i), (l) 64-dimensional case with $\kappa_1 = 1$. Hamiltonian of (a)∼(f) can be found in Eq. (III), Hamiltonian of (g)∼(l) can be found in[46,47].